Soluble Star-Shaped Molecules Based on Thiophene Derivatives as Organic Semiconductors for Field-Effect Transistor Applications

Kyung Hwan Kim,[†] Zhenguo Chi,[†,§] Min Ju Cho,[†] Jung-Il Jin,[†] Mi Yeon Cho,[‡] Su Jin Kim,[‡] Jin-soo Joo,[‡] and Dong Hoon Choi*,[†]

Department of Chemistry, Center for Electro- & Photo-responsive Molecules, and Department of Physics, Korea University, Seoul 136-701, South Korea

Received July 4, 2007

New star-shaped crystalline molecules have been synthesized through Horner-Emmons reactions using hexyl-substituted thiophene-based carbaldehydes as dendrons and [1,2,4,5-tetra-(diethoxy-phosphoryl-methyl)-benzyl]-phosphonic acid diethyl ester as the core units; these molecules have been fully characterized. Three thiophene-based star-shaped molecules exhibit good solubility in common organic solvents and good self-film-forming properties. They are intrinsically crystalline as they exhibit well-defined X-ray diffraction patterns from uniform and preferred orientations of molecules. The semiconducting properties of the star-shaped molecules have been evaluated in organic field-effect transistors. Three crystalline conjugated molecules, **4**, **8**, and **12**, exhibit carrier mobilities as high as 6.0 ($\pm$0.5) $\times$ 10^{-3}, 2.5 ($\pm$0.5) $\times$ 10^{-4}, and 2.5 ($\pm$0.5) $\times$ 10^{-2} $cm^2 \cdot V^{-1} \cdot s^{-1}$, respectively. The dithienothiophene dendrons in **12** induce easy crystallization and small crystallite formation even in as-cast films and can be found to densely cover the surface of a dielectric layer. This helps in attaining good network interconnection of the carrier transport channel, which is responsible for the relatively high carrier mobility in solution-processed organic semiconductors for OFET.

Introduction

Soluble organic semiconducting materials based on extended π-conjugated systems have received considerable attention for electronic devices over the last several years. Among various kinds of soluble organic semiconducting materials, star-shaped crystalline molecules have been highlighted to be synthesized because of their strong potential applications to organic field-effect transistors (OFETs)[1−5] and organic photovoltaic devices.[6−8]

Compared with linear organic conjugated oligomers and polymers used in OFETs, star-shaped molecules have a number of advantages including the ability to demonstrate multifunctionality in one molecule. The synthesis of π-conjugated star-shaped molecules raises the possibility of creating thiophene derivatives that are fully tethered to the aromatic core. Furthermore, the solubility problem in conjugated linear oligothiophene is totally overcome under a star-shaped architecture. Recently, star-shaped molecules have been developed as an interesting class of semiconducting materials and hence, thus far, there are only a few reports about their application in field-effect transistors.[1−5] Ponomarenko et al. first reports the synthesis of three-armed star-shaped oligothiophenes which demonstrated successful semiconducting characteristics for solution-processible OFETs.[1] Sun et al. also reported the OFET devices performances of the oligothiophene-functionalized truxene derivatives that are star-shaped polycyclic compounds.[2] The devices fabricated by spin coating displayed the highest mobility up to 1.03 $\times$ 10^{-3} $cm^2/V \cdot s$ and which is 1 order of magnitude higher than the first one reported by Ponomarenko et al. Although more star-shaped molecules are also developed to investigate OFET characteristics, the reported soluble star-shaped molecules that bear three conjugated arms exhibit relatively low carrier mobilities (μ = 1.0 $\times$ 10^{-5} to 1.0 $\times$ 10^{-3} $cm^2 \cdot V^{-1} \cdot s^{-1}$).[1−4]

The most promising performance for an OFET device made of star-shaped oligothiophene was reported by Ponomarenko et al.[5] They linked oligothiophenes through flexible aliphatic branches to a carbosilane core. The highest performance exhibited by a spin-coated sample on SiO_2 treated with octyldimethylchlorosilane was a linear mobility of 1.2 $\times$ 10^{-2} $cm^2/V \cdot s$ with an on/off ratio of 1 $\times$ 10^5. To the best of our knowledge, no device performance was better than the one above for an OFET that is made of soluble star-shaped molecules and has been reported thus far.

* Corresponding author. E-mail: dhchoi8803@korea.ac.kr.
† Department of Chemistry, Center for Electro- & Photo-responsive Molecules.
§ Present address: School of Chemistry and Chemical Engineering, Sun Yat-sen University, Guangzhou 510275, PRC.
‡ Department of Physics.

(1) Ponomarenko, S. A.; Kirchmeyer, S.; Elschner, A.; Huisman, B.-H.; Karbach, A.; Drechsler, D. *Adv. Funct. Mater*. **2003**, *13*, 591−596.
(2) Sun, Y.; Xiao, K.; Liu, Y.; Wang, J.; Pei, J.; Yu, G.; Zhu, D. *Adv. Funct. Mater*. **2005**, *15*, 818−822.
(3) Sonntag, M.; Kreger, K.; Hanft, D.; Strohriegl. *Chem. Mater.* **2005**, *17*, 3031−3039.
(4) Cravino, A.; Roquet, S.; Alévêque, O.; Leriche, P.; Frére, P.; Roncali, J. *Chem. Mater.* **2006**, *18*, 2584−2590.
(5) Ponomarenko, S. A.; Tatarinova, E. A.; Muzafarov, A. M.; Kirchmeyer, S.; Brassat, L.; Mourran, A.; Moeller, M.; Setayesh, S.; De Leeuw, D. *Chem. Mater.* **2006**, *18*, 4101−4108.
(6) De Bettignies, R.; Nicolas, Y.; Blanchard, P.; Levillain, E.; Nunzi, J.-M.; Roncali, J. *Adv. Mater*. **2003**, *15*, 1939−1943.
(7) Cremer, J.; Bäuerle, P. *J. Mater. Chem.* **2006**, *16*, 874−884.
(8) Roquet, S.; Cravino, A.; Leriche, P.; Alévêque, O.; Frére, P.; Roncali, J. *J. Am. Chem. Soc.* **2006**, *128*, 3459−3466.

10.1021/cm071760c CCC: $37.00
Published on Web 08/24/2007

In this study, we prepared crystallizable star-shaped molecules containing bithiophene, thienothiophene, and dithienothiophene as dendritic wedges. We employed the Horner-Emmons method rather than Heck and Suzuki coupling methods to tether the dendritic wedges to the core, which is free from transition metal catalyst. [1,2,4,5-Tetra-(diethoxy-phosphorylmethyl)-benzyl]-phosphonic acid diethyl ester was used as the core unit for the new semiconducting dendritic molecules. We investigated the optical properties, thermal properties, electrochemical properties, and photophysical properties of the new star-shaped molecules. A closely packed molecular arrangement in the annealed films is expected in view of the structural packing observed by the X-ray diffraction method. OFETs based on these molecules have been fabricated by a simple drop-casting method on bare silicon oxide. Three crystalline conjugated molecules, **4**, **8**, and **12**, exhibited saturated carrier mobilities as high as 6.0 ($\pm$0.5) $\times$ 10^{-3}, 2.5 ($\pm$0.5) $\times$ 10^{-4}, and 2.5 ($\pm$0.5) $\times$ 10^{-2} $cm^2 \cdot V^{-1} \cdot s^{-1}$, respectively.

Experimental Details

Synthesis. Detailed synthetic procedures for all compounds and characterization data can be found in the Supporting Information.

Compounds **1**, **2**, **5**, **6**, **9**, **10**, and [1,2,4,5-tetra-(diethoxy-phosphorylmethyl)-benzyl]-phosphonic acid diethyl ester as a core unit were synthesized by following the literature method and a modified method.[9−15]

Instrumental Analysis. ^{1}H NMR spectra were recorded on a Varian Mercury NMR 300 Hz spectrometer using deuterated chloroform purchased from Cambridge Isotope Laboratories, Inc. Elemental analyses were performed using an EA1112 (Thermo Electron Corp.) elemental analyzer. MALDI-TOF analysis was performed on a Voyager-DE STR MADI-TOF (matrix; DHB) mass spectrometer. High-resolution mass analysis was performed on a JMS-700 MStation mass spectrometer (JEOL, resolution 60,000, *m*/*z* range at full sensitivity 2400).

Thermal properties were studied under a nitrogen atmosphere on a Mettler DSC 821^e instrument. Thermal gravimetric analysis (TGA) was conducted on a Mettler TGA50 (temperature rate 10 °C/min under N_2). The redox properties of star-shaped molecules were examined by using cyclic voltammetry (Model: EA161 eDAQ). Thin films were coated on a platinum plate using chloroform as a solvent. The electrolyte solution employed was 0.10 M tetrabutylammonium hexafluorophosphate (Bu_4NPF_6) in a freshly dried MC. The Ag/AgCl and Pt wire (0.5 mm in diameter) electrodes were utilized as reference and counter electrodes, respectively. The scan rate was at 50 mV/s. X-ray diffraction (XRD) experiment was performed at varying temperatures using the synchrotron radiation (1.542 Å) of the 3C2 beam line at the Pohang Synchrotron Laboratory, Pohang, Korea. The film samples were fabricated by drop-casting on silicon wafer, followed by drying at 70 °C under vacuum (solvent: chloroform, concentration of the solution: 10 mg/mL).

The measurements were obtained in a scanning interval of 2θ between 1° and 40°. Atomic force microscopy (Digital Instruments Multimode equipped with a nanoscope IIIa controller) operating in tapping mode with a silicon cantilever was used to characterize the surface morphologies of the samples. The film samples were fabricated by spin coating (1500 rpm) on silicon wafer followed by drying at 40 °C under vacuum (solvent: chloroform, concentration of the solution: 10 mg/mL).

Absorption and Photoluminescence (PL) Spectroscopy. To study absorption behavior, the films of three molecules were fabricated on quartz substrates as follows. The solution (3 wt %) of each molecule in monochlorobenzene was filtered through an acrodisc syringe filter (Millipore 0.2 μm) and subsequently spin-cast on the quartz glass. The films were dried overnight at 70 °C for 48 h under vacuum.

Absorption spectra of samples in a film and solution state (chloroform, concentration 1 $\times$ 10^{-5} mol/L) were obtained using a UV−vis spectrometer (HP 8453, photodiode array type) in the wavelength range of 190−1100 nm. PL spectra of the solutions were acquired on an AMINCO-Bowman series-2 luminescence spectrometer.

OFET Fabrication. Bottom-contact OFET devices were fabricated using the gold source and drain electrodes which were thermally evaporated using the conventional method. A p-doped polycrystalline silicon was used as a gate electrode with its 250 nm bare SiO_2 surface layer used as a gate dielectric insulator. The gold was deposited onto the untreated SiO_2 surface via thermal evaporation. A 400 nm thick film of the semiconductor layer was deposited at 25 °C by drop-casting a 2 wt % solution of star-shaped molecule in monochlorobenzene. Then it was dried and annealed at a certain temperature for 1−0.5 h. The device characteristics of the FETs were measured with Keithley 237 source meters, with the samples in an ambient atmosphere.

Results and Discussion

Synthesis. We report here the facile and high-yield synthesis of the new p-type thiophene-based star-shaped semiconducting molecules. Scheme 1 illustrates the synthetic routes for the dendritic molecules, **4**, **8**, and **12**. The four-armed crystalline star-shaped molecules contain bithiophene, thienothiophene, or dithienothiophene as the dendritic wedge. For instance, a hexyl group is attached to [2,2′]bithiophenyl using 1-bromohexane via cold lithiation. **2**, **6**, and **10** undergo a low-temperature kinetic formylation reaction, which is used to produce the corresponding carbaldehydes. In our previous synthesis, we employed the Heck coupling method for **4** and **8**.[16] **4** was prepared by palladium-catalyzed Heck reaction of 5-hexyl-5′-vinyl-[2,2′]bithiophenyl and 1,2,4,5-tetrabromobenzene. Compared to Horner-Emmons reaction, the reaction yield is relatively very small around 20−30%. Horner-Emmons coupling of [1,2,4,5-tetra-(diethoxy-phosphorylmethyl)-benzyl]-phosphonic acid diethyl ester and thiophene-based carbaldehyde produces the conjugated star-shaped molecules **4**, **8**, and **12** with a yield of 76−86%.

The resulting material is then purified by silica-gel column chromatography or reprecipitation into ethanol. The identity

(9) Wei, Y.; Yang, Y.; Yeh, J.-M. *Chem. Mater.* **1996**, *8*, 2659−2666.
(10) Fuller, L. S.; Iddon, B.; Smith, K. A. *J. Chem. Soc., Perkin Trans.* **1997**, *1*, 3465−3470.
(11) Frey, J.; Bond, A. D.; Holmes, A. B. *Chem. Commun.* **2002**, 2424−2425.
(12) De Jong, F.; Janssen, M. J. *J. Org. Chem.* **1971**, *36*, 1645−1648.
(13) Li, X.-C.; Sirringhaus, H.; Garnier, F.; Holmes, A. B.; Moratti, S. C.; Feeder, N.; Clegg, W.; Teat, S. J.; Friend, R. H. *J. Am. Chem. Soc.* **1998**, *120*, 2206−2207.
(14) Gerold, J.; Holzenkamp, U.; Meier, H. *Eur. J. Org. Chem.* **2001**, *2001*, 2757−2763.
(15) Meier, H.; Fetten, M. *Tetrahedron Lett.* **2000**, *41*, 1535−1538.
(16) Kim, K. H.; Chi, Z.; Cho, M. J.; Choi, D. H.; Kang, H. S.; Cho, M. Y.; Joo, J.-S. *Appl. Phys. Lett.* **2006**, *89*, 202109(1)−202109(3).

Scheme 1. Synthesis of the Star-Shaped Crystalline Molecules[a]

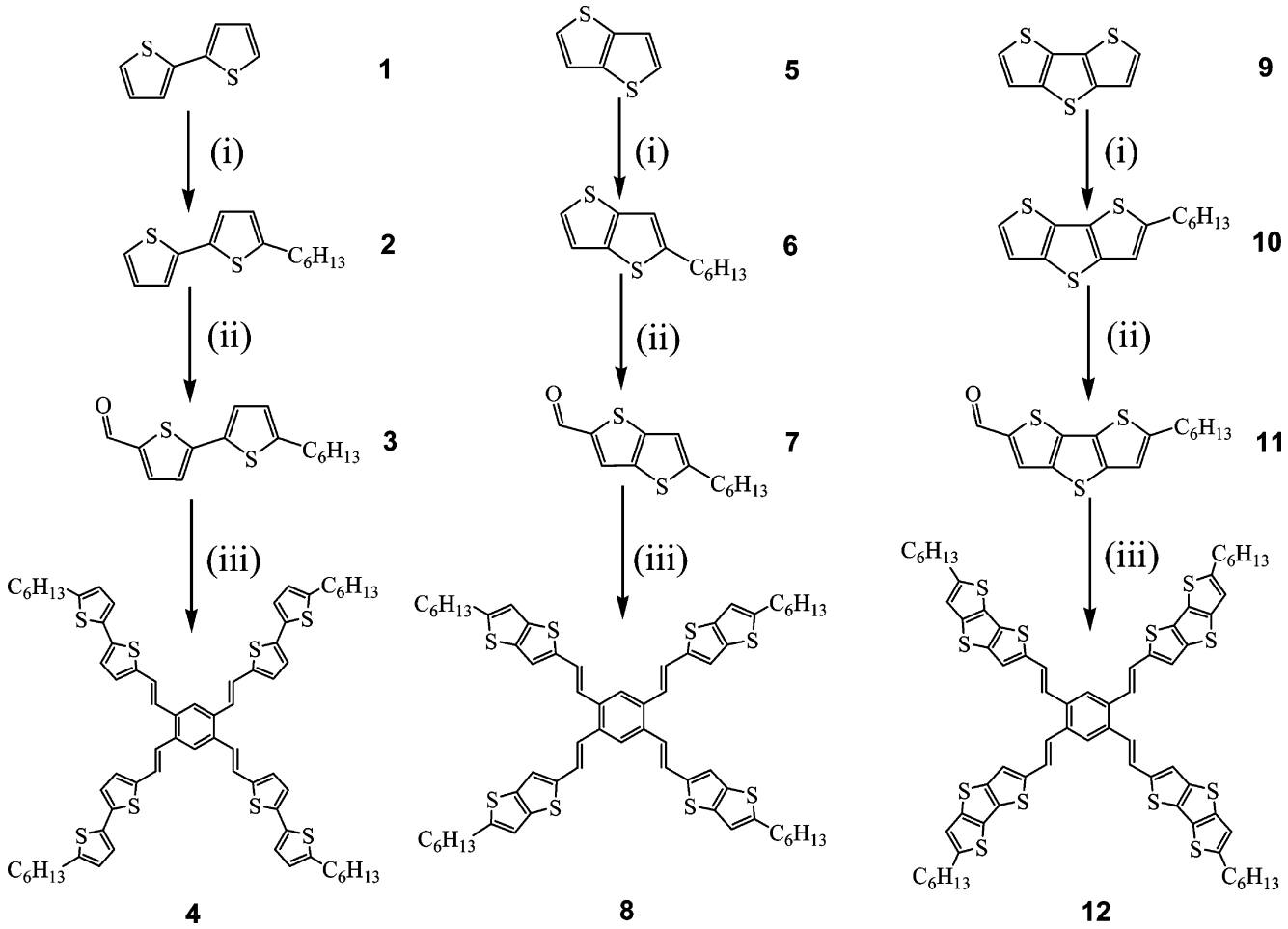

[a] (i) 1-Bromohexane, *n*-BuLi, THF, rt; (ii) *n*-BuLi, DMF, THF, −78 °C; (iii) [1,2,4,5-tetra-(diethoxy-phosphorylmethyl)-benzyl]-phosphonic acid diethyl ester, potassium *tert*-butoxide, THF, rt.

and purity of the synthetic materials were confirmed by ^{1}H NMR, HRMS, MALDI-TOF mass spectrometry, and elemental analysis. They were found to have good self-film-forming properties and were well-soluble in various organic solvents such as chloroform, xylene, MC, chlorobenzene, and THF.

In particular, in comparison to the solubility (about <1 mg/mL) of α,α′-dihexyl sexithiophene (DH-6T) in monochlorobenzene, their solubility proved to be considerably better. More than 40, 34, and 15 mg of **4**, **8**, and **12**, respectively, are soluble in 1 mL of monochlorobenzene.

Thermal Analysis. When we employ the star-shaped molecules for OFET applications, their thermal stabilities and dynamic behaviors are emphasized for device fabrication. The thermal properties of the star-shaped molecules were characterized by differential scanning calorimetry (DSC) and thermogravimetric analysis (TGA). DSC measurement was performed at a heating (cooling) scan rate of 10 (−10) °C/min under nitrogen with the highest temperature limited to below the decomposition temperature. **4** and **8** exhibit distinct crystalline-isotropic transitions at 178 and 172 °C, respectively. One endothermic peak at 90 °C in **8** is thought to be a cold crystallization temperature. **12** exhibits a broad melting temperature range from 240 °C. This thermogram indicates that **12** undergoes thermal decomposition just after melting (see Figure 1A). TGA measurements at a heating rate of 10 °C/min under nitrogen revealed that the star-shaped molecules had good thermal stabilities. Compared to the onset decomposition temperature of DH-6T, which is at around 309 °C, these crystalline molecules have enhanced onset decomposition temperatures (∼350−380 °C), as shown in Figure 1B.

Although the temperature was raised up to 900 °C, some residual weights were measured in **8** and **12**, which are attributed to the char formation from a fused ring structure of the peripheral dendrons.

Optical and Photoluminescence (PL) Properties. The absorption spectra of the samples in chloroform (concentration 1×10^{-5} mol/L) and thin films were obtained (see Figure 2). The absorption maxima of **4**, **8**, and **12** in solution state are located at 422, 395, and 426 nm, respectively. **8** exhibits a lower λ_{max} due to its shorter intramolecular conjugation length than others. We observe a drastic spectral change in the film states of **4** and **12**, which is attributed to a high degree of intermolecular interaction. For instance, in the thin film of **4** after annealing at 150 °C, the absorption spectrum is significantly red-shifted with clear vibronic transitions at 443 (480) and 516 nm, which are attributed to

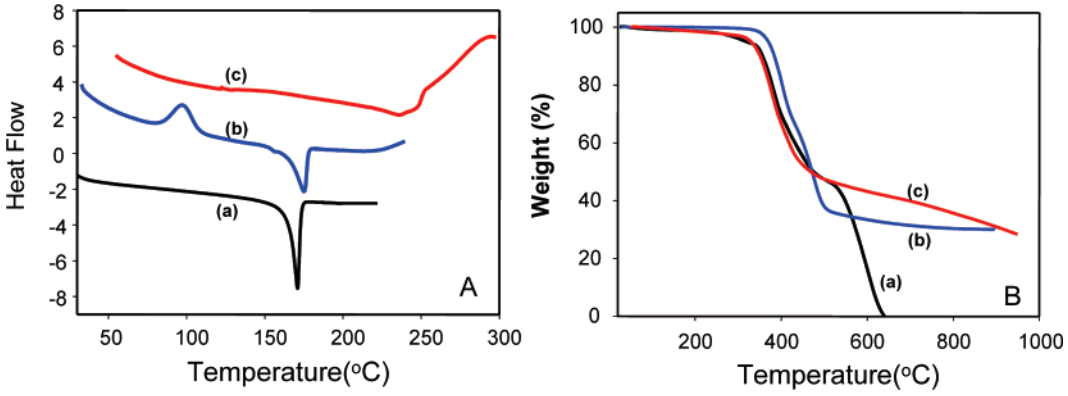

Figure 1. DSC and TGA thermograms of **4** (a), **8** (b), and **12** (c) recorded at a ramp rate of 10 °C /min. A: DSC; B: TGA.

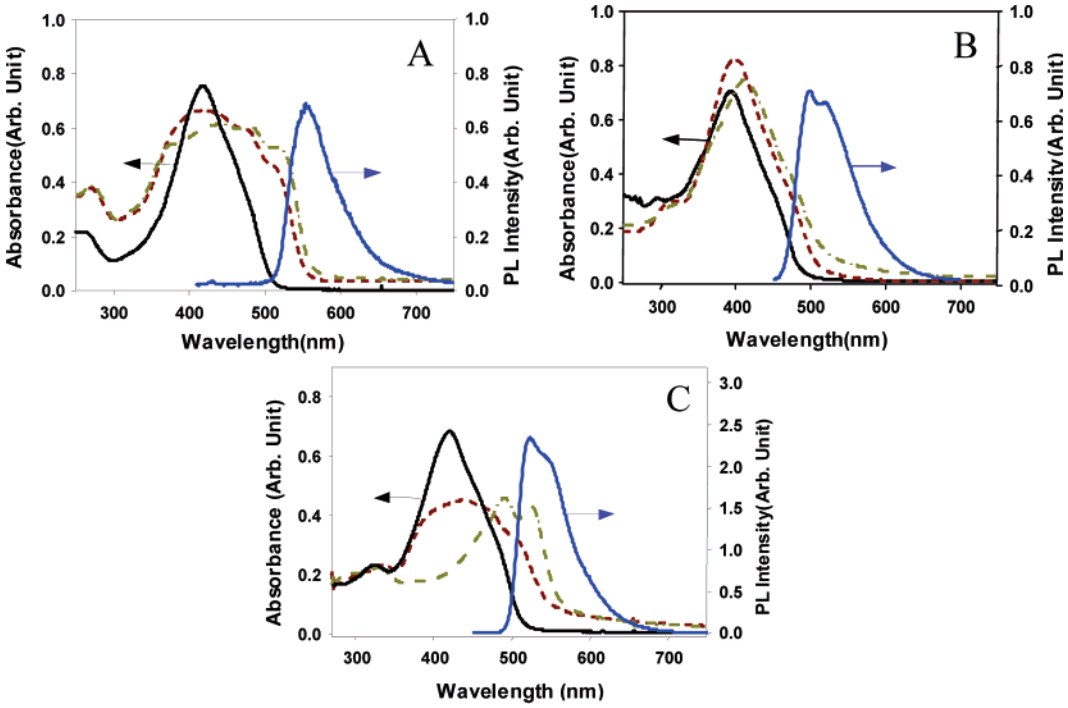

Figure 2. Optical absorption (UV/vis) and emission (PL) spectra of **4** (A), **8** (B), and **12** (C). The PL spectrum of the film was obtained by exciting at 400 nm. *(Solid line) solution, (dashed line) pristine film, (dash-dot-dashed line) annealed film. PL spectra were taken in solution states.

the formation of an ordered structure with an intermolecular π-stacking[1,2,17] (see Figure 2A).

The greater resolution in **12** may have resulted from a denser and more rigid molecular packed structure in the crystalline domain. However, the vibronic absorption peaks of the thin film of **8** are not discernible, possibly due to the small extent of the intermolecular interaction.

Although the HOMO−LUMO gaps (ΔE_2s) in the crystalline films were not accurately determined by absorption spectroscopy, the difference (ΔE_3) between the HOMO−LUMO gaps in solution and film states provides useful information in understanding the intermolecular interactions. The HOMO−LUMO gaps of the solution and annealed film are tabulated in Table 1. The difference in the HOMO−LUMO gap in solution state results from the difference in the intramolecular conjugation through the core. The larger difference (ΔE_3) (=0.20 and 0.22 eV) in **4** and **12** imply a higher degree of intermolecular interaction in the film states.

Table 1. HOMO−LUMO Gaps of Star-Shaped Molecules in a Solution and Film State

	ΔE_1 (eV)[a]	ΔE_2 (eV)[b]	ΔE_3 (eV)[c]
4	2.40	2.20	0.20
8	2.54	2.40	0.14
12	2.42	2.20	0.22

[a] ΔE_1: HOMO−LUMO gap of solution sample in chloroform. [b] ΔE_2: HOMO−LUMO gap of annealed film sample. [c] $\Delta E_3 = \Delta E_1 - \Delta E_2$.

The three star-shaped molecules, **4**, **8**, and **12**, exhibit featureless PL spectral behaviors with emission maxima at 554, 498 (519), and 523 (552) nm, respectively, as seen in Figure 2. The PL emission maxima show a bathochromic shift with increasing conjugation lengths. The longer conjugation length in **4** and **12** induces the distinct red-shifted emission wavelength, while **8** and **12** show two PL emission wavelengths, possibly due to the vibronic structure that is typical for oligothiophenes.[18,19] The PL spectra reveal smaller Stokes shifts for **8** (ca. 0.083 eV) and **12** (ca. 0.078 eV) than

(17) Pei, J.; Wang, J.-L.; Cao, X.-Y.; Zhou, X.-H.; Zhang, W.-B. *J. Am. Chem. Soc.* **2003**, *125*, 9944−9945.

(18) Facchetti, A.; Yoon, M. H.; Stern, C. L.; Hutchison, G. R.; Ratner, M. A.; Marks, T. J. *J. Am. Chem. Soc.* **2004**, *126*, 13480−13501.

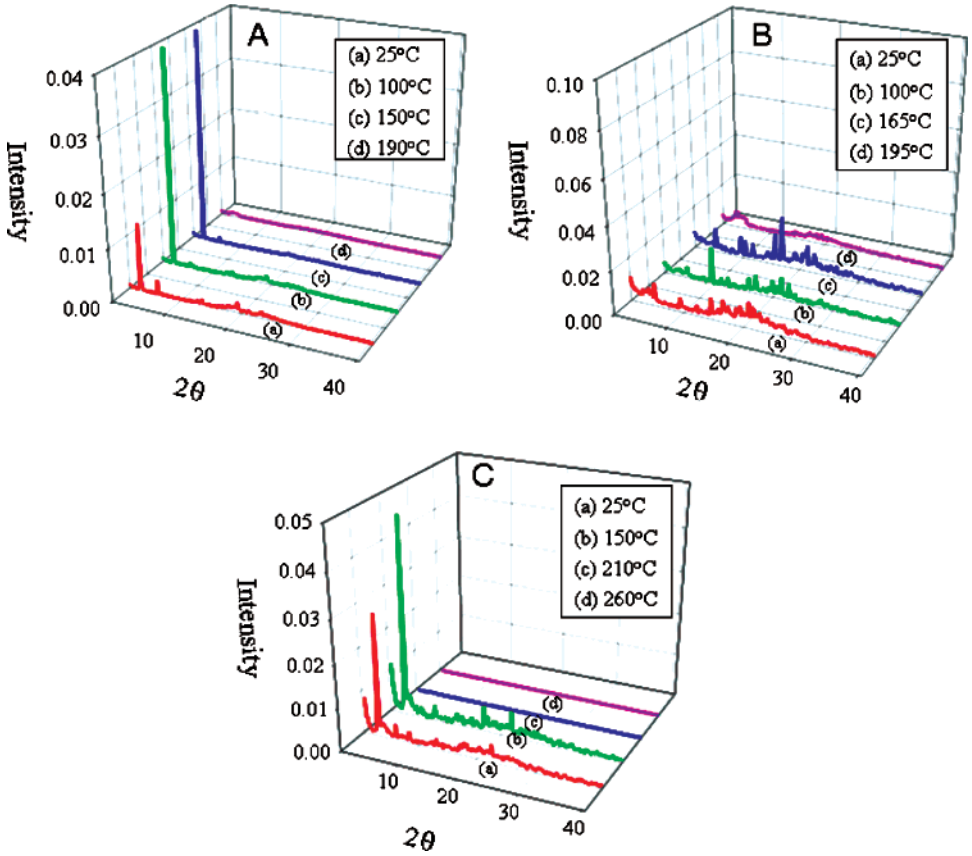

Figure 3. Temperature dependence of X-ray diffraction patterns of (A) **4**, (B) **8**, and (C) **12**. The spectrum recorded at each temperature corresponds to a film grown at the temperature for 5 min.

Table 2. Physical Properties of the Three Star-Shaped Molecules and Device Performance of OFET

	T_m (°C)	T_d (°C)	$\lambda_{max}^{abs.}$ (nm)[a]	E_g^{opt} (eV)[b]	$\lambda_{max}^{em.}$ (nm)[a]	energy level HOMO (eV)[b]	energy level LUMO (eV)[b]	μ_{max} ($cm^2/V \cdot s$)	I_{on}/I_{off}
4	178	345	422	2.20	557	−5.19	−2.99	$6.0 (\pm 0.5) \times 10^{-3}$	$>10^4$
8	172	350	395	2.40	497, 521	−5.17	−2.77	$2.5 (\pm 0.5) \times 10^{-4}$	$\sim 10^3$
12	247	332	426	2.20	523, 547	−5.25	−3.05	$2.5 (\pm 0.5) \times 10^{-2}$	$>10^3$

[a] Solution sample in chloroform. [b] Film sample.

for **4** (ca. 0.090 eV), consistent with a lesser structural reorganization on photoexcitation due to a more rigid ground state geometry. This implies that thienothiophene or dithienothiophene induces planarity in the molecules and self-rigidification.

Electrochemical Analysis. Electrochemical characterization of these molecules as films evidenced that their oxidation is reversible, which is a necessary condition for a FET active material. The values of the ionization potential match well with the work function of a gold electrode. Cyclic voltammograms were recorded on a film sample and the potentials were obtained relative to an internal ferrocene reference (Fc/Fc^+). These CV scans in the range of −2.0 to +2.0 V (vs Ag/AgCl) range show quasi-reversible oxidation peaks. Unfortunately, the reduction behaviors were irreversible; therefore, we were unable to accurately estimate their HOMO and LUMO energies. To determine the LUMO levels, we combined the oxidation potential in CV with the optical energy band gap (E_g^{opt}) resulting from the absorption edge in the absorption spectrum. Voltammograms of **4**, **8**, and **12** in the film state show that their lowest oxidative waves are at +0.79, +0.77, and +0.85 V, respectively.

As shown in Table 2, **4**, **8**, and **12** have HOMO levels of −5.19, −5.17, and −5.25 eV, respectively. The relatively higher HOMO level of **12** should endow the material with better environmental stability. In addition, **4**, **8**, and **12** have LUMO energy levels of −2.99, −2.77, and −3.05 eV, respectively.

X-ray Diffraction Analysis. To study the crystallinity and preferred orientations of the star-shaped molecules, X-ray diffraction (XRD) was performed with varying temperatures. The star-shaped molecular layers must be associated with the layered stacking properties brought about by the terminal alkyl groups, which are already known to induce long-range ordering. X-ray diffraction scans of films of **4**, **8**, and **12** annealed at different temperatures reveal the temperature at which the highest crystalline order is achieved (see Figure 3). In the film samples made of **4** and **12**, the preferred orientation is clearly inferred through the high reflection intensity of the peaks at 30 Å ((100) reflection) and the

(19) Facchetti, A.; Deng, Y.; Wang, A.; Koide, Y.; Sirringhaus, H.; Marks, T. J.; Friend, R. H. *Angew. Chem., Int. Ed.* **2000**, *39*, 4547−4551.

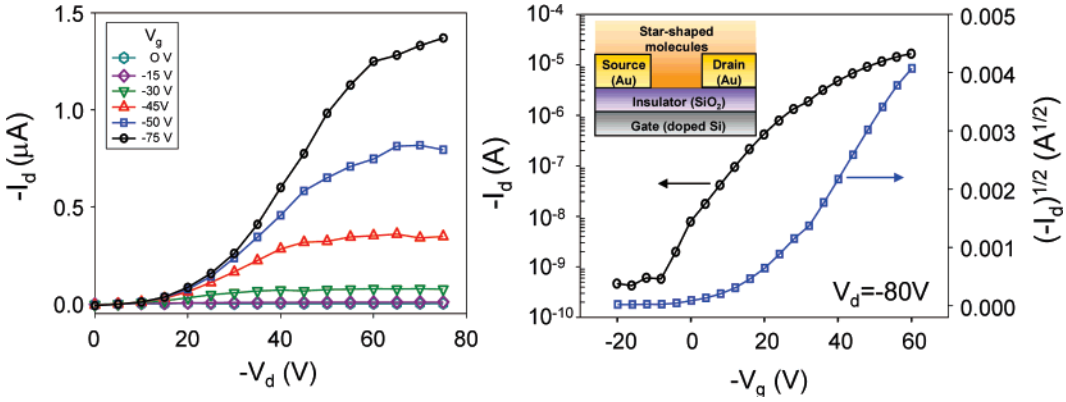

Figure 4. Output (left) and transfer (right) characteristics of OFET made by the drop-casting of **4** from monochlorobenzene solution, annealed at 150 °C for 30 min.

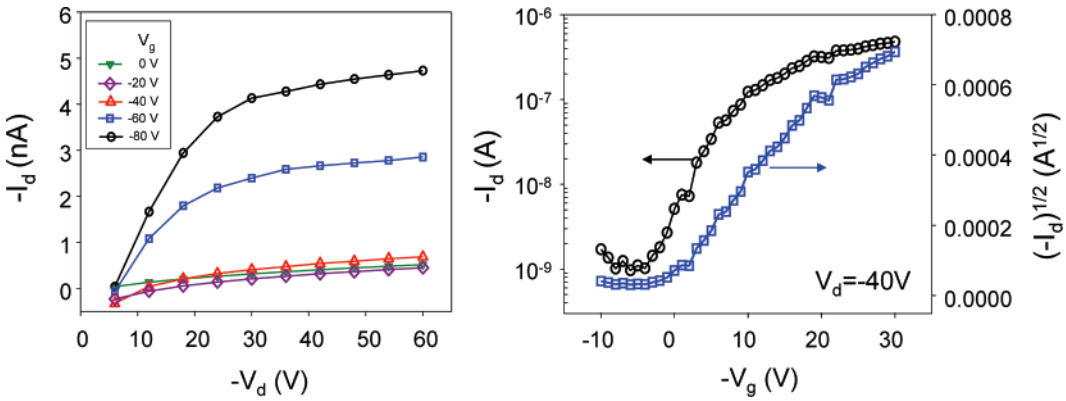

Figure 5. Output (left) and transfer (right) characteristics of OFET made by the drop-casting of **8** from monochlorobenzene solution, annealed at 100 °C for 30 min.

presence of peaks in the 3−5 Å ((010) reflection) region, as seen in our X-ray diffractograms. The former spacing corresponds to the edge-to-edge transverse packing of the peripheral arms and the latter to a $\pi-\pi$ stacked distance having a π-electron cloud overlap. **4** and **12** exhibited a large increment in the intensity of the (100) reflection after annealing. However, the intensity of the (010) reflection reduced slightly. This result implies that most of the crystallites in **4** and **12** are preferentially oriented along the (100)-axis in the plane.

In the case of **8**, there is some ambiguity in determining the exact long-range spacing in a small angle region. No discernible (100) reflection was observed; the intensity of the (010) reflection was dominant, although some polycrystalline morphology was observed.

Therefore, we consider the orientation of **8** to be parallel to the surface with a face-on or a random structure. This morphological behavior may affect the interlayer carrier transport property in an FET device made of **8**.

Aside from the vacuum evaporation technique, it has been suggested that it is difficult to achieve high crystallinity for the films of organic molecules. However, in our solution-processed films, significantly high crystalline properties and the preferential orientation of the ordered molecular domains were found in the samples made of **4** and **12**.[2,20,21]

Properties of OFET Made of Star-Shaped Molecules. Bottom-contact OFET devices were fabricated using gold source and drain electrodes which were thermally evaporated using the conventional method. p-Doped polycrystalline silicon was used as the gate electrode, with a 250 nm bare SiO_2 surface layer used as the gate dielectric insulator. The gold was deposited onto the *unmodified* SiO_2 surface via thermal evaporation. A 400 nm thin film of the semiconductor was deposited by drop-casting a 2 wt % solution of the molecules in monochlorobenzene. To achieve the optimal performance, the OFET devices made of **4**, **8**, and **12** were further annealed at 150, 100, and 150 °C, respectively, for 30 min. The output characteristics showed very good saturation behaviors and clear saturation currents that were quadratic to the gate bias (see Figures 4, 5, and 6). The saturated field-effect mobilities, μ_{FET}, can be calculated from the amplification characteristics, by using the classical equations describing field-effect transistors.[22] The mobility values obtained by measuring five different devices are listed in Table 2.

The transistor devices of **4**, **8**, and **12** provided a field-effect mobility of 2.0×10^{-4} to 3.0×10^{-2} $cm^2 \cdot V^{-1} \cdot s^{-1}$ together with a high current on/off ratio and a low threshold voltage ($V_{th} < -15$ V). Among the three star-shaped molecules, **12** showed the highest mobility. We could obtain the carrier mobility as high as 3.0×10^{-2} $cm^2 \cdot V^{-1} \cdot s^{-1}$ for

(20) Garnier, F.; Yassar, A.; Hajlaoui, R.; Horowitz, G.; Deloffre, F.; Servet, B.; Ries, S.; Alnot, P. *J. Am. Chem. Soc.* **1993**, *115*, 8716−8721.
(21) Wu, R.; Schumm, J. S.; Pearson, D. L.; Tour, J. M. *J. Org. Chem.* **1996**, *61*, 6906−6921.
(22) Merlo, J. A.; Newman, C. R.; Gerlach, C. P.; Kelley, T. W.; Muyres, D. V.; Fritz, S. E.; Toney, M. F.; Frisbie, C. D. *J. Am. Chem. Soc.* **2005**, *127*, 3997−4009.

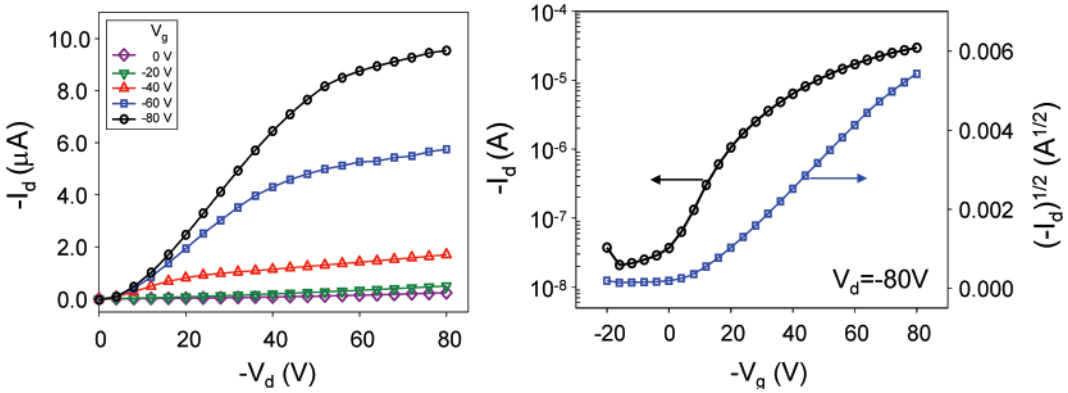

Figure 6. Output (left) and transfer (right) characteristics of OFET made by the drop-casting of **12** from monochlorobenzene solution, annealed at 150 °C for 30 min.

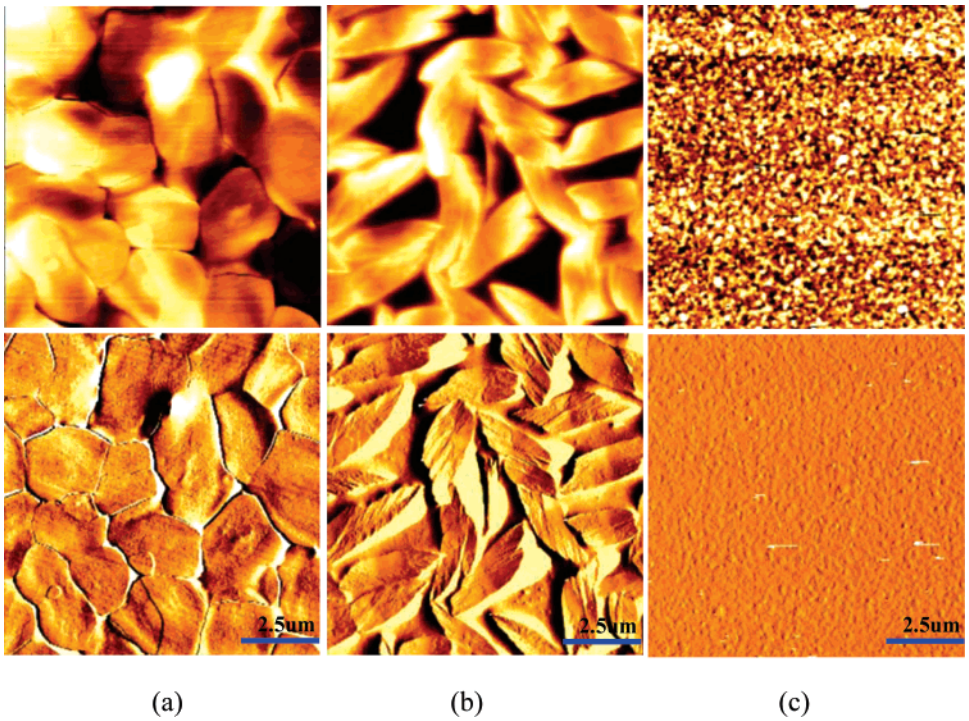

Figure 7. AFM height (upper) and phase (lower) images (10 μm $\times$ 10 μm). (a) **4**; (b) **8**; (c) **12**.

a 20 μm channel length device, although the current on/off ratio is slightly lower than 10^3.

Our optical spectroscopy and XRD results could provide indirect evidence of the strong intermolecular interaction and preferred molecular orientation of **12** in the crystalline film. Therefore, the predominant edge-on orientation of **4** and **12** can explain the higher value of the field-effect mobilities as compared to that of **8** which exhibits a random orientation of the molecules.

To explain why **12** exhibits the highest mobility, we investigated the surface coverage of the dielectric layer using AFM. In addition to the long-range molecular structural organization confirmed by X-ray study, the AFM micrographs display well-resolved surface structures on the dielectric layer.

Therefore, we analyzed the topography and phase image of the semiconducting layer on the SiO_2 layer. We prepared the solution of each molecule and then performed spin coating to cover the dielectric surface with each solution. After complete drying, we took three sets of micrographs as shown in Figure 7.

Among the three molecules, **12** shows the compact structure on the surface with the smallest crystallites. **4** and **8** are comprised of larger crystallites than **12**. A high coverage of the substrate is achieved simply by spin coating of **12**. It can be thought that the highly packed crystalline molecules on the dielectric layer can help the carrier transport with good connection behavior. The novel star-shaped architecture provides a clear confirmation of the considerable improvement in charge-transport efficiency obtained.

Conclusions

We have successfully synthesized and characterized new star-shaped crystalline molecules that are solution-processable. They show good film-forming properties and a high degree of crystallinity. Upon UV−vis absorption spectroscopy, the intermolecular interaction between the molecules can be tuned by thermal annealing processes, which changes

the electronic properties. **12** not only forms smooth films on large surfaces but also shows better homogeneous layer formation with relatively small crystallites. In addition to the molecular arrangement on the substrate in a predominant edge-on manner, the small crystallites of **12** cover the substrate uniformly and with good network interconnection between the crystallites, which is probably responsible for the moderately high carrier mobility in the solution-processed organic semiconductors for OFET. To the best of our knowledge, no mobility higher than that for soluble **12** ($\mu = 2.0-3.0 \times 10^{-2}$ cm^2/V·s) has been reported in the class of star-shaped molecules and conjugated dendrimers. The improved solution processability and high field-effect mobility make **12** the best candidate for a promising new class of semiconducting materials for future flexible electronics. The surface treatment of the polymeric dielectric layer is now underway to enhance the field-effect mobility and the other device performances. Most recently, we treated the surface of SiO_2 with octadecyltrichlorosilane (OTS) and fabricated the OFET with **12**. The maximum mobility was found to be around 6.0 ($\pm$0.5) $\times 10^{-2}$ cm^2/V·s with a poor on/off ratio of 2.0 $\times 10^2$. The devices with a self-assembled interlayer are being optimized to improve their performances and reproducibility.

Acknowledgment. This research work was supported by 21st century Frontier Research Program (F0004091-0000-00) and LG-Philips-LCD CO. Ltd (2006-2007). Particularly, M. J. Cho acknowledges the financial support by the Seoul R&BD Program (2006−2007). X-ray experiments at PLS were supported by the Ministry of Science and Technology and Pohang Steel Company.

Supporting Information Available: Detailed procedures for the synthesis as well as spectrometric characterization of the compounds reported (PDF). This material is available free of charge via the Internet at http://pubs.acs.org.

CM071760C